Chinese Chemical Letters 35 (2024) 109291

Contents lists available at ScienceDirect

Chinese Chemical Letters

journal homepage: www.elsevier.com/locate/cclet

Enzymatically controlled DNA tetrahedron nanoprobes for specific imaging of ATP in tumor

Xiaohong Wen[1], Mei Yang[1], Lie Li, Mingmin Huang*, Wei Cui, Suping Li, Haiyan Chen, Chen Li, Qiuping Guo*

College of Biology, State Key Laboratory of Chemo/Biosensing and Chemometrics, College of Chemistry and Chemical Engineering, Key Laboratory for Bio-Nanotechnology and Molecular Engineering of Hunan Province, Hunan University, Changsha 410082, China

ARTICLE INFO

Article history:
Received 4 September 2023
Revised 6 November 2023
Accepted 7 November 2023
Available online 10 November 2023

Keywords:
Enzyme-controlled
APE1
DNA tetrahedron
Cancer-specific
ATP biosensing

ABSTRACT

Intracellular ATP is an emerging biomarker for cancer early diagnosis because it is a key messenger for regulating the proliferation and migration of cancer cells. However, the conventional ATP biosensing strategy is often limited by the undesired on-target off-tumor interference. Here, we reported a novel strategy to design enzymatically controlled DNA tetrahedron nanoprobes (En-DT) for biosensing and imaging ATP in tumor cells. The En-DT was designed *via* rational engineering of structure-switching aptamers with the incorporation of an enzyme-activatable site and further conjugation on the DNA tetrahedron. The En-DT could be catalytically activated by apurinic/apyrimidinic endonuclease 1 (APE1) in cancer cells, but they did not respond to ATP in normal cells, thereby enabling cancer-specific ATP biosensing and imaging *in vitro* and *in vivo* with improved tumor specificity. This strategy would facilitate the precise detection of a broad range of biomarker in tumors and may promote the development of smart probes for cancer diagnosis.

Adenosine triphosphate (ATP) is the direct source of energy and is needed to organize all life activities of cells in living organisms [1]. As a multifunctional biological organic phosphate, ATP plays an important role in many physiological processes such as energy storage, cellular respiration, signal transduction, enzyme catalysis, and muscle contraction [2–5]. It has reported that the abnormal increment of ATP level in the organism is often closely related to many pathological processes, such as inflammation, anemia, and malignant tumors [6–8]. In many kinds of cancers, ATP plays a vital role in regulating the proliferation and migration of cancer cells, so ATP can be used as a cancer biomarker for research [9,10]. Therefore, it is important to develop a tool to effectively detect intracellular ATP for the early diagnosis of cancer.

In particular, various aptamer-based DNA nanodevices have been designed for ATP detection in test-tubes or living cells, as they possess high programmability and biocompatibility [11–19]. Several strategies have been explored to confer stimulus-responsive behavior to aptamers for conditional control of their functions. For example, it has been reported that aptamer activity can be pH-responsive upon fusion with i-motif sequences [20,21]. Hypoxia-sensitive aptamers are regulated by chemical modifications to modulate their binding to cell surface targets [22]. However, ATP aptamer can be activated during the cellular delivery and uptake process and impede the visualize the ATP level in tumor cells. The structural properties of the ATP aptamer may be artificially damaged, resulting in genome instability and hindrance to binding to ATP. Hence, it is necessary to design a reliable strategy for ATP imaging in tumor. In recent years, the DNA tetrahedron performs large amounts of advantages, such as nanoscale controllability, low cytotoxicity, excellent cellular permeability, and high digestion-resistant ability [23–25]. It showed good application prospects in anti-digestion, sensor construction, and biological imaging [26–31]. Therefore, the development of endogenous molecular-activated aptamer-based DNA tetrahedron nanoprobes is more attractive for the detection of ATP in tumor cells.

Apurinic/apyrimidinic endonuclease 1 (APE1), a key enzyme that catalyzes the hydrolysis of apurinic/apyrimidinic (AP) sites in the base excision repair (BER) process, was chosen as the enzyme trigger [32]. Studies have shown that APE1 exists predominantly in the nucleus in normal cells but is overexpressed in the cytosolic region in cancer cells [33–35]. APE1-activated aptamer-based DNA tetrahedron nanoprobes may enable tumor-specific biosensing and imaging.

* Corresponding authors.
E-mail addresses: huangxiaoqin@hnu.edu.cn (M. Huang), guoqping@hnu.edu.cn (Q. Guo).
[1] These authors contributed equally to this work.

https://doi.org/10.1016/j.cclet.2023.109291
1001-8417/

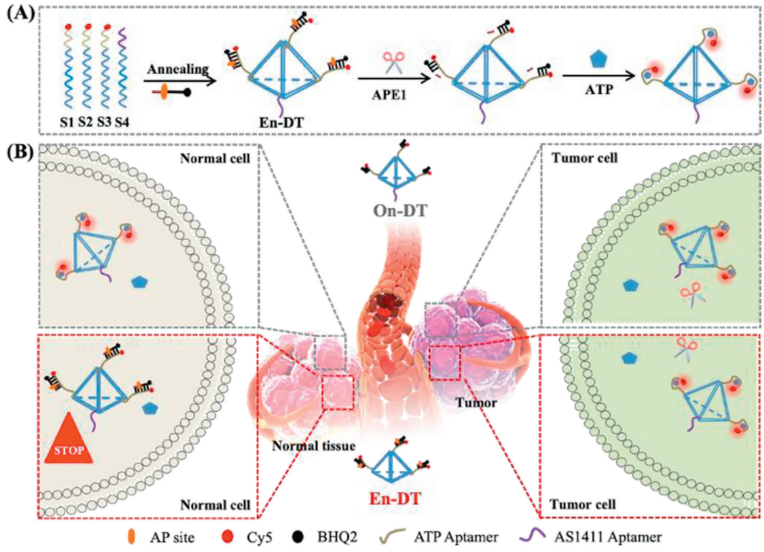

Fig. 1. (A) Schematic illustration of the enzyme-triggered ATP sensing mechanism of En-DT. (B) Locked En-DT could be activated by APE1 in tumor cells for ATP sensing, while the on-target off-tumor response in normal cells was inhibited, leading to improved tumor specificity compared with the conventional structure-switching nanoprobes (On-DT, which possessed the same structure as En-DT except that the L2-AP-Q was replaced with L2-Q). The gray box was the detection effect of On-DT probe, while the red box was the detection effect of En-DT.

Thus motivated, here we presented the design of an enzyme-controlled, aptamer-based DNA tetrahedron nanoprobe (denoted as En-DT), which was established *via* rational reengineering of conventional structure-switching aptamer by incorporation of an enzyme activation unit and further conjugation of the aptamer targeting action (ATP aptamer and AS1411) on the DNA tetrahedron (Fig. 1). First, the DNA tetrahedron (DT) framework [31] was constructed from four oligonucleotides (S1, S2, S3, and S4), in which S1, S2, and S3 are appended with ATP aptamer with modification of Cy5 at the 3′-end, while the oligonucleotides S4 are extended with AS1411 aptamer. Next, a complementary DNA strand (L2-AP-Q) containing an AP site spaced 13 nucleotides at the 5′-end, which yields a low fluorescence background due to the fluorescence resonance energy transfer (FRET) between the dye Cy5 and quencher BHQ_2 labeled on ATP aptamer and L2-AP-Q, respectively (Fig. 1A). Furthermore, the formation of a duplex structure of En-DT can suppress the recognition capability of the aptamer to ATP in normal cells, leading to the "locked" sensing activity (Fig. 1B). In the presence of APE1, the AP site will be recognized and catalytically cleaved to generate a single nucleotide gap in L2-AP-Q, producing short DNA strands and a less stable duplex structure. Therefore, the ATP aptamer will restore its structure-switching capability to bind ATP and lead to the dissociation of BHQ_2 on the cleaved L2-AP-Q and thus a fluorescence enhancement for ATP detection. We envision that the enzyme-triggerable DNA tetrahedron nanoprobes allow for ATP sensing with improved tumor specificity in comparison with conventional structure-switching nanoprobes (On-DT).

Formation of the En-DT was verified by 2% agarose gel electrophoresis. As shown in Fig. 2A, lanes 2, 3, 4, 5, and 6 showed the strands of S1, S1 + S2, S1 + S2 + S3, S1 + S2 + S3 + S4 (DT), and S1 + S2 + S3 + S4 + L2-AP-Q (En-DT), respectively. With the addition of strands from lane 2 to lane 6, lane 6 (En-DT) migrated slower than the other lanes because of the high molecular weight of the En-DT. This result indicated that the En-DT were formed successfully. Moreover, dynamic light scattering (DLS) was used to confirm the formation of the En-DT, which is shown in Fig. 2B, through measuring the size of the En-DT. The result showed that the hydrodynamic size increased from 10.81 ± 1.2 nm for DT to 13.63 ± 0.9 nm for En-DT, indicating successful anchoring of the responsive unit onto the DT framework. Thus, both the agarose gel

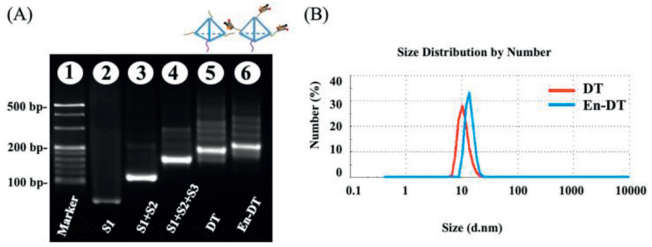

Fig. 2. (A) Validation of En-DT by 2% agarose gel electrophoresis: lane 1, Marker; lane 2, S1; lane 3, S1 + S2; lane 4, S1 + S2 + S3; lane 5, S1 + S2 + S3 + S4; lane 6, S1 + S2 + S3 + S4 + L2-AP-Q. (B) DLS analysis of DT and En-DT. Nanoprobe concentration was 50 nmol/L.

electrophoresis and DLS results confirmed the successful fabrication of the En-DT.

The enzyme-controlled performance of En-DT was evaluated in buffer. When only ATP or APE1 was added to the buffer, no significant fluorescent signal was detected (Fig. 3A and Fig. S1 in Supporting information). However, in the presence of both ATP and APE1, the enzyme-controlled En-DT was activated, resulting in the change of conformation from "locked" to "free" state, which was necessary for specific binding of ATP and the recovery of fluorescence signal, as evidenced by the significant increase in the Cy5 fluorescence intensity at 633 nm. These results indicated that our engineered En-DT probe has potential for ATP detection in tumor cells.

To verify the activation mechanism, a conventional ATP sensor (On-DT) which containing a complementary sequence (L2-Q) was designed as a control. Upon the addition of ATP, On-DT showed a significantly increased fluorescence intensity, while En-DT displayed a negligible signal (Fig. S2 in Supporting information), indicating the locked sensing activity of En-DT through the engineering with the APE1-activated part. As another control, we constructed a control probe (nEn-DT) with the same structure as En-DT but without the AP site. Minimum fluorescence signal alteration was observed for nEn-DT in the presence of APE1 and ATP (Fig. 3B), revealing that the modification of the AP site was a prerequisite for the design. Furthermore, it showed that En-DT exhibited a good selectivity to APE1 against other enzyme (Fig. S3 in Supporting in-

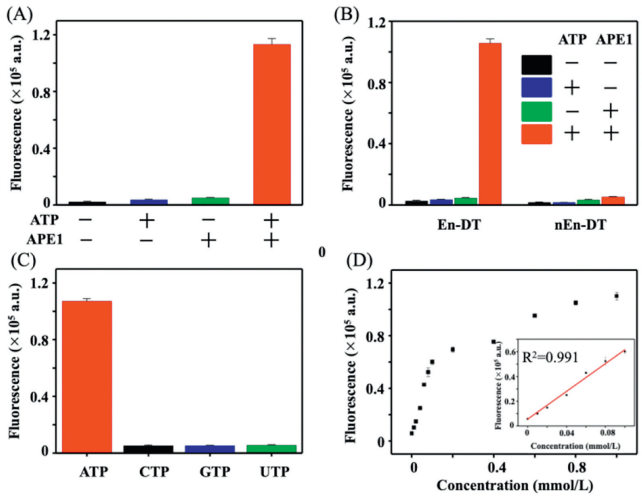

Fig. 3. (A) Fluorescence intensity of En-DT responding to ATP (5 mmol/L) with or without APE1 activation (1 U/mL). (B) Fluorescence intensity of En-DT (50 nmol/L), and nEn-DT responding to ATP (5 mmol/L) with or without APE1 activation (1 U/mL). (C) Selectivity of En-DT toward different analytes (5 mmol/L) with APE1 activation (1 U/mL). (D) Fluorescence intensity of the En-DT treated with different concentrations of ATP (0–1 mmol/L). Data are represented as means ± SD, $n = 3$. Nanoprobe concentration was 50 nmol/L.

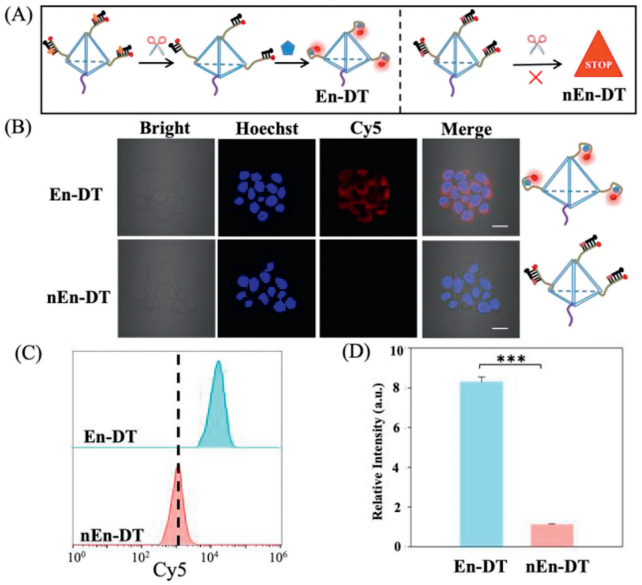

Fig. 4. (A) Schematic showing ATP sensing mechanism of En-DT and nEn-DT, respectively. (B) Fluorescence images of MCF-7 cells treated with En-DT and nEn-DT, respectively. MCF-7 cells were stained with Hoechst 33342 (blue). Scale bar: 20 μm. (C) Flow cytometric assay of MCF-7 cells incubated with En-DT and nEn-DT, respectively. (D) Quantitative flow cytometric results of the fluorescence signal ratio of Cy5 to MCF-7 cells treated with En-DT and nEn-DT, respectively. Data are means ± SD ($n = 3$). $^{***}P < 0.001$. Nanoprobe concentration was 50 nmol/L.

formation). Also, the addition of UTP, CTP, or GTP did not display any fluorescence response (Fig. 3C and Fig. S4 in Supporting information).

Further, to evaluate the response ability of the En-DT to the ATP, the fluorescence intensities of En-DT to different concentrations of ATP were measured. Fig. S5 (Supporting information) showed that fluorescence intensities of the En-DT enhanced gradually with the increasing concentration of the ATP from 0 to 1 mmol/L, testifying that the fluorescence recovery of En-DT was due to the binding between aptamer and ATP. Additionally, Fig. 3D shows that the fluorescence intensity of Cy5 was linearly proportional to ATP concentration ranging from 0 to 1 mmol/L ($R^2 = 0.991$). The results proved that En-DT has good ability to respond to ATP. Furthermore, the response kinetics of the En-DT to target ATP was studied by real-time monitoring fluorescence signal. When both ATP and APE1 exist, as shown in Fig. S6 (Supporting information), the fluorescence signal recovered slowly after 10 min incubation and gradually enhanced with the increase of incubation time. The fluorescence signal tended to balance at 100 min. However, when either ATP or APE1 was missing, no significant fluorescence signal was observed, indicating that the En-DT nanoprobe required the synergistic activation of ATP and APE1, and indicating that this strategy can quickly respond to ATP in solution, which was conducive to the specific detection of ATP in living cells.

The DNA tetrahedron could protect the aptamer from degradation under cellular circumstances. As shown in Fig. S7 (Supporting information), the En-DT could remain integrated after being incubated with the medium containing 10% fetal bovine serum (FBS) at 37 °C for 9 h, indicating that the En-DT has good stability in serum biological samples and can be used for long-term imaging analysis of ATP in living cells. Then, the efficient cellular uptake of En-DT in MCF-7 cells was confirmed by the imaging study and flow cytometry assay of Cy5-labeled E-Apt-Cy5 (E-Apt-Cy5, which possessed Cy5 labeled ATP aptamer and L2-AP-Q) and En-DT-Cy5 (En-DT-Cy5, which possessed the same structure as En-DT except that the L2-AP-Q was not labeled with the BHQ_2) (Fig. S8 in Supporting information). The colocalization study showed that En-DT-Cy5 localized partially in the cytoplasm after the uptake, while double-stranded E-Apt-Cy5 probe could hardly enter cells autonomously, verifying that the En-DT has better cell internalization ability (Fig. S9 in Supporting information). Moreover, the biocompatibility investigation with cell counting kit-8 (CCK-8) assay showed that En-DT were not cytotoxic to cells (Fig. S10 in Supporting information).

Then, we investigated the ability of En-DT to image intracellular ATP in tumor cells MCF-7. The En-DT was found to produce strong fluorescence signal, while the control probe (nEn-DT) induced much weaker fluorescence (Figs. 4A and B), suggesting that the observed signal of En-DT resulted from dual activatable imaging. In addition, the flow cytometric quantification showed that En-DT displayed about 7.5-fold higher fluorescence intensity than that of nEn-DT (Figs. 4C and D). To further confirm that the signal indeed come from the dual activatable response, we pretreated MCF-7 cells with IAA (a glycolysis inhibitor that could cause ATP depletion) to down-regulate the ATP level before imaging with the En-DT [36]. Inspection of the cell images showed that the fluorescence signal decreased significantly (Fig. S11 in Supporting information). We further used NCA, an APE1 inhibitor, to reduce the APE1 level [37]. Similarly, the imaging data showed significantly diminished fluorescence signal in the treated cells (Fig. S12 in Supporting information). Collectively, these results confirmed the enzymatically gated ATP sensing activity of the En-DT.

We then evaluated the capability of En-DT to differentiate between normal cells and cancer cells. By comparison, L02 cells were chosen as the control normal cells to evaluate the cell specificity of ATP sensing. As expected, a minimal Cy5 fluorescent signal of En-DT was observed in L02 cells treated with the same amount of En-DT for the same time because of the lack of APE1 in the cytosol of normal cells (Fig. S13 in Supporting information). In contrast, both the MCF-7 cells and L02 cells showed comparatively strong fluorescence when treated with the conventional probe (On-DT), confirming that the overexpression of APE1 in cancer cells played a key role in improving the cell specificity of ATP sensing (Fig. S13). Furthermore, we verified that the En-DT was applicable for cancer-specific ATP sensing in other cancer cell lines (Fig. S14 in Supporting information). Collectively, the results indicated that

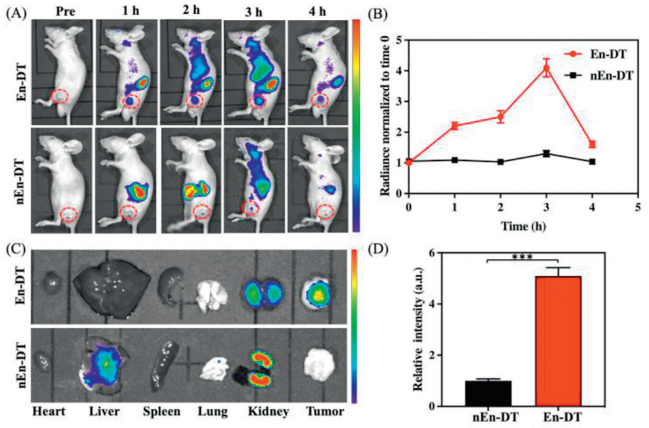

Fig. 5. (A) Fluorescence imaging of MCF-7 tumor-bearing mice i.v. injected with En-DT, On-DT and nEn-DT. (B) Quantitative fluorescence intensity in tumors according to (A). (C) Fluorescence images of *ex vivo* organs and tumors harvested at 3 h after i.v. injection of different systems. (D) Quantitative fluorescence intensity in tumors according to (C). Data are mean ± SD, $n = 3$. $^{***}P < 0.001$. Nanoprobe concentration was 1.5 μmol/L.

the enzyme-controlled DNA tetrahedron nanoprobes allowed for cancer-cell-specific molecular sensing.

We then studied its tumor-specific ATP imaging capability *in vivo*. All the animal operations followed the institutional animal use and care regulations according to protocol, approved by the Laboratory Animal Center of Hunan Province (No. SCXK (Xiang) 2018–0006). Nude mice bearing MCF-7 xenograft tumors were randomly intravenously injected with En-DT and nEn-DT and subjected to *in vivo* imaging. A significant increase in fluorescence signal was observed in the tumor region 3 h post injection for the mice treated with En-DT (Figs. 5A and B). On the contrary, a negligible increase in fluorescence contrast was observed over the same time frame for the nEn-DT treated group, suggesting that the enhanced fluorescence signal at the tumor site in the En-DT group was due to the enzyme-triggered ATP sensing. The enzyme-activated ATP imaging was further validated by comparing the fluorescence signals of harvested tumors and organs 3 h postinjection (Fig. 5C). The result showed that the intratumoral fluorescence signal in the En-DT group was significantly higher than that in the nEn-DT group. Quantitative analysis revealed that the mean intratumoral fluorescence intensity in the En-DT group was about 5.1-fold higher than that in the groups receiving nEn-DT (Fig. 5D). The high fluorescence signals in the kidneys of different groups could be attributed to the gradual clearance of DNA molecules through the renal route [38], as generally observed for diverse nucleic acid delivery systems and DNA-based probes [39,40]. These results confirmed that the En-DT allowed for enzyme-activated ATP sensing *in vivo*.

In summary, we developed a novel strategy to design enzyme-triggered DNA tetrahedron nanoprobes for ATP biosensing with improved cancer specificity. The En-DT could be selectively activated in tumor cells by APE1, which restored its structure-switching capability to bind and sense intracellular ATP. Compared with the conventional On-DT, the enzyme-activatable En-DT displayed enhanced signal contrast in the tumor by suppressing the background fluorescence from normal tissues, resulting in an improved tumor specificity. In addition, En-DT has good biocompatibility and the ability to enrich in tumor. It has been successfully used in living cells (MCF-7, A549 and HeLa cells) and mice to monitor ATP levels by fluorescence imaging. It is expected that the En-DT for intracellular ATP will become an effective tool for cancer early diagnosis in clinic. Moreover, this enzyme-triggered strategy would facilitate the construction of diverse nanodevice for sensing other cellular targets and might promote precise cancer diagnosis.

Declaration of competing interest

The authors declare that they have no known competing financial interests or personal relationships that could have appeared to influence the work reported in this paper.

Acknowledgment

This work was supported by the National Natural Science Foundation of China (Nos. 21877030, 21735002, 21778016).

Supplementary materials

Supplementary material associated with this article can be found, in the online version, at doi:10.1016/j.cclet.2023.109291.

References

[1] M.T. Lin, M.F. Beal, Nature 443 (2006) 787–795.
[2] A. Patel, L. Malinovska, S. Saha, Science 365 (2017) 753–756.
[3] P.B. Dennis, A. Jaeschke, M. Saitoh, et al., Science 294 (2001) 1102–1105.
[4] J.R. Knowles, Annu. Rev. Biochem. 49 (1980) 877–919.
[5] J.H. Young, J. Mclick, E.F. Korman, Nature 249 (1974) 474–476.
[6] M.I. Sweeney, Neurosci. Biobehav. Rev. 21 (1997) 207–217.
[7] T. Foltynie, Lancet Neurol. 18 (2019) 1072–1074.
[8] D.C. Wallace, Science 283 (1999) 1482–1488.
[9] E. Adinolfi, L. Raffaghello, A.L. Giuliani, et al., Cancer Res. 72 (2012) 2957–2969.
[10] S.M. Gilbert, C.J. Oliphant, S. Hassan, Oncogene 38 (2018) 194–208.
[11] D.E. Huizenga, J.W. Szostak, Biochemistry 34 (1995) 656–665.
[12] D. Zheng, D.S. Seferos, D.A. Giljohann, et al., Nano Lett. 9 (2009) 3258–3261.
[13] Y. Xiang, Y. Lu, Nat. Chem. 3 (2011) 697–703.
[14] Z. Liu, S. Chen, B. Liu, et al., Anal. Chem. 86 (2014) 12229–12235.
[15] H.K. Walter, J. Bauer, J. Steinmeyer, et al., Nano Lett. 17 (2017) 2467–2472.
[16] J. Zhao, J. Gao, W. Xue, et al., J. Am. Chem. Soc. 140 (2018) 578–581.
[17] X. Meng, H. Wang, M. Yang, et al., Anal. Chem. 93 (2021) 1693–1701.
[18] Z. Xiang, J. Zhao, D. Yi, et al., Chem. Int. Ed. 60 (2021) 22659–22663.
[19] D. Zhao, D. Chang, Q. Zhang, et al., J. Am. Chem. Soc. 143 (2021) 15084–15090.
[20] A.E. Rangel, A.A. Hariri, M. Eisenstein, et al., Adv. Mater. 32 (2020) 2003704.
[21] I.V. Nesterova, E.E. Nesterov, J. Am. Chem. Soc. 136 (2014) 8843–8846.
[22] F. Zhou, T. Fu, Q. Huang, et al., J. Am. Chem. Soc. 141 (2019) 18421–18427.
[23] N. Xie, J. Huang, X. Yang, et al., ACS Sensors 1 (2016) 1445–1452.
[24] Z. Ge, H. Gu, Q. Li, et al., J. Am. Chem. Soc. 140 (2018) 17808–17819.
[25] L. He, D. Lu, H. Liang, et al., J. Am. Chem. Soc. 140 (2018) 258–263.
[26] Z. Liu, H. Pei, L. Zhang, et al., ACS Nano 12 (2018) 12357–12368.
[27] K. Zhang, W. Huang, Y. Huang, et al., Anal. Chem. 91 (2019) 7086–7096.
[28] Y. Zhang, Y. Deng, C. Wang, et al., Chem. Sci. 10 (2019) 5959–5966.
[29] W. Fan, B. Yung, P. Huang, et al., Chem. Rev. 117 (2017) 13566–13638.
[30] S.G. Harroun, C. Prevost-Tremblay, D. Lauzon, et al., Nanoscale 10 (2018) 4607–4641.
[31] L. Li, J. Wang, H.S. Jiang, et al., Chin. Chem. Lett. 34 (2023) 107506.
[32] D. Yi, J. Zhao, L. Li, Angew. Chem. Int. Ed. 60 (2021) 6300–6304.
[33] C.D. Mol, T. Izumi, S. Mitra, et al., Nature 403 (2000) 451–456.
[34] F. Shah, D. Logsdon, R.A. Messmann, et al., NPJ Precis. Oncol. 1 (2017) 19.
[35] S. Choi, H.K. Joo, B.H. Jeon, Chonnam Med. J. 52 (2016) 75–80.
[36] J. Verrax, N. Dejeans, B. Sid, et al., Biochem. Pharmacol. 82 (2011) 1540–1548.
[37] M.L. Fishel, M.R. Kelley, Mol. Aspects Med. 28 (2007) 375–395.
[38] R.L. Juliano, Nucl. Acids Res. 44 (2016) 6518–6548.
[39] R. Yan, J. Chen, J. Wang, et al., Small 14 (2018) 1802745.
[40] X. Zhu, B. Qu, Z.M. Ying, et al., Anal. Chem. 92 (2020) 15953–15958.